Physics Letters A 181 (1993) 296–307
North-Holland

PHYSICS LETTERS A

Violation of the semi-classical approximation and quantum chaos in a paramagnetic spin system

Gennady P. Berman [a,b], Evgeny N. Bulgakov [a,b], Darryl D. Holm [a,c] and Vladimir I. Tsifrinovich [b]

[a] *Center for Nonlinear Studies, MS-B258, Los Alamos National Laboratory, Los Alamos, NM 87545, USA*
[b] *Kirensky Institute of Physics, Research and Educational Center for Nonlinear Processes at Krasnoyarsk Polytechnical Institute, and Theoretical Department at Krasnoyarsk State University, 660036 Krasnoyarsk, Russian Federation*
[c] *Theoretical Division, MS-B284, Los Alamos National Laboratory, Los Alamos, NM 87545, USA*

Received 26 May 1993; accepted for publication 6 August 1993
Communicated by A.R. Bishop

Quantum effects are considered in the dynamics of a system of N paramagnetic atoms in a resonant cavity interacting with a constant magnetic field and with a resonant external magnetic field. In the semi-classical limit (classical radiation field in the cavity) this resonantly driven system shows developed (global) chaos. Expectation-value dynamics shows however that quantum corrections cause a departure from the semi-classical chaotic dynamics on a time-scale $\tau_\hbar \sim \ln N$ and that quantum correlation functions grow exponentially in time. The possibility of experimentally observing this effect is discussed.

1. Introduction

A fundamental problem in quantum chaos of Hamiltonian systems is to determine how significantly quantum effects cause a system's dynamics to depart from its corresponding classical chaotic motion, starting from the same initial conditions and for parameter values in the quasiclassical region. This problem is fundamental in quantum mechanics [1] but, for quantum *nonintegrable* systems, the methods needed to deal with it are still being developed. Investigations of this problem have been carried out during the last few years on rather simple models [2–10] with one-and-a-half degrees of freedom. These investigations have shown that when "developed" dynamical chaos appears in the classical limit the quasiclassical approximation is violated in logarithmically small times, $\tau_\hbar \sim \ln \kappa$ (where $\kappa = \text{const}/\hbar$ is the quasiclassical parameter). This means that for early times ($\tau < \tau_\hbar$) quantum dynamics only differs slightly from its corresponding classical motion, but at later times ($\tau > \tau_\hbar$) quantum effects become significant. So, at times of order $\tau_\hbar$ the character of the dynamics of the quantum system begins making a qualitative departure from its corresponding classical chaotic motion. We call time $\tau_\hbar$ at which this happens the classical/quantum crossover time scale for the system.

Experiments carried out recently with Rydberg states of hydrogen atoms in microwave fields investigate processes such as electron diffusion up to the ionisation threshold [11–13]. However, even for initial populations of electrons prepared with fairly large principal quantum number, $n \sim 50$–100, such systems cannot be considered quasiclassical enough to observe the classical/quantum crossover time scale, $\tau_\hbar$; since in this case the time scale $\tau_\hbar$ is too small for current experimental techniques to measure. On the other hand, most systems in which classical nondissipative chaos may be observed are so macroscopic that their time scale $\tau_\hbar$ exceeds all characteristic relaxation times. Consequently, the classical/quantum crossover time at which the transition from classical nondissipative chaotic motion to quantum dynamics occurs cannot be observed in these systems either. This problem is related to the general problem of validity of quantum mechanics for the description of big "classical" systems. It is known that

0375-9601/93/$ 06.00 © 1993 Elsevier Science Publishers B.V. All rights reserved.

usually the time $\tau_\hbar$ when quantum corrections finally must be taken into account to describe the dynamics of a big "classical" system significantly exceeds any relaxation times for the system, and sometimes even exceeds the age of the universe. Thus, between these two extremes the problem arises, to identify systems for which the transition from classical Hamiltonian chaos to essentially quantum dynamics may be experimentally observed.

In this paper we consider a system whose classical/quantum transition may turn out to be experimentally observable. The system consists of N paramagnetic spins ($s=\frac{1}{2}$) placed in a resonator with large quality factor, Q. These spins interact with an external spatially homogeneous magnetic field, B_0. We assume there is no direct interaction between the spins. Their interaction is solely through a single electromagnetic eigenmode of the resonator, and this mode is chosen to be in resonance with the frequency $\omega=g\mu_B B_0/\hbar$ of spin precession in the external magnetic field B_0. In this part of the problem formulation, our system is analogous to the quantum Dicke model [14–16], well known in nonlinear optics, which describes cooperative effects in an ensemble of N two-level atoms in a single-mode resonant cavity. We then add to our spin system a periodically modulated magnetic field, perpendicular to B_0, with spatially uniform amplitude b_0 and with modulation frequency Ω slightly different from the eigenmode frequency (or the spin precession frequency ω). This field acts on the spins as a nearly-resonant periodic external force. We show that three characteristic frequencies appear in the slow dynamics of this system: (1) the cooperative Dicke frequency ω_c which describes slow self-consistent energy exchange between the spins and the resonator eigenmode; (2) the Rabi frequency ω_R which is proportional to the amplitude b_0 of the external magnetic field and describes slow nutation of an individual spin in resonance with the periodically varying external magnetic field; and (3) the difference $\Delta=\omega-\Omega$ between the frequency of spin precession in the magnetic field B_0 and the frequency of the external coherent magnetic field. In the semi-classical approximation (when the radiation field in the resonator is considered as a classical sub-system) this system shows "developed" (global) chaos under conditions that may be expressed roughly as follows: $\omega_c \sim \omega_R \sim |\Delta|$. This condition means that in slow dynamics the different nonlinear resonances strongly interact. We take into account quantum effects by treating the eigenmode of the resonator as a quantum linear oscillator. In this quantum system, the action of the self-consistent field (eigenmode) is big: $I_{\text{field}} \sim \hbar N \gg \hbar$ and the system is in the "deep" quasi-classical region.

The main result of the paper is the following: for this spin system in the parameter region where developed chaos occurs in the semi-classical approximation, quantum effects lead to violation of the semi-classical description on the time scale $\tau_\hbar \sim \ln N$. Moreover, in this case quantum correlation functions grow exponentially during the time before $\tau_\hbar$, at a rate that may be experimentally measurable. The paper is organized as follows. Section 2 describes the paramagnetic spin model. In section 3 the Hamiltonian for the slow dynamics of the spin model is derived. Section 4 presents an exact c-number equation for the slow dynamics of quantum expectation values in a coherent-state representation of this model. Section 5 discusses the semi-classical approximation and gives some new results on the semi-classical chaos shown by this model system. Section 6 shows numerical simulations of the effects of quantum corrections on semi-classical chaotic dynamics in this model system obtained using the c-number equation presented in section 4. In the conclusion, we discuss the experimental measurability of these effects.

2. Description of the paramagnetic spin model

We consider fixed in a material sample N paramagnetic atoms, each with spin one-half, placed in a cavity resonator and interacting self-consistently via a single resonator eigenmode. These spins also interact with an externally imposed, homogeneous, magnetic field with two orthogonal components, B_0 and $b(t)$. The first of these, B_0, is constant and has its spin precession frequency tuned to the frequency of the resonator eigenmode. The other homogeneous external magnetic field component, $b(t)$, is modulated periodically in time, with modulation frequency slightly detuned from that of the resonator eigenmode (see fig. 1).

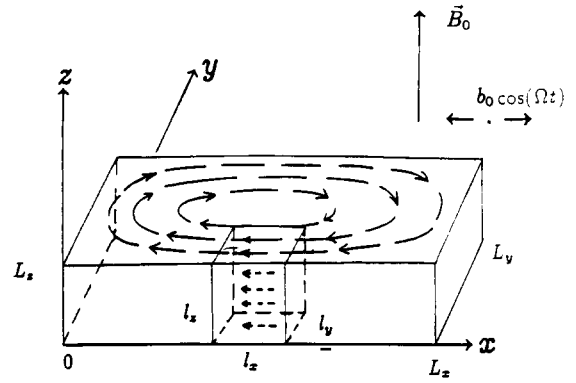

Fig. 1. Rectangular resonator with linear dimensions L_x, L_y, L_z and a paramagnetic sample with dimensions $l_x \ll L_x$, $l_y \ll L_y$, $l_z = L_z$. A constant magnetic field B_0 is directed along the z axis; a periodic magnetic field $b_0 \cos(\Omega\tau)$ is linearly polarized along the x axis. The curves show the distribution of magnetic field in a chosen resonator eigenmode (this field is homogeneous in the z direction).

We assume we can excite in the cavity resonator a single eigenmode, characterized by its eigenfrequency $\omega = 2\pi f$ and by the geometry of its electric and magnetic field lines. Thus, the amplitudes of all other modes are taken to be negligibly small in comparison with the amplitude of the excited mode. The frequency of magnetic resonance is determined by the constant external magnetic field, B_0, and may be tuned to match the frequency of the excited eigenmode. For example, in electron paramagnetic resonance (PMR) assuming $B_0 = 1$ kOe and $g = 2$ gives

$$f = \frac{g\mu_B B_0}{2\pi\hbar} \sim 3 \text{ GHz} .$$

The amplitude of the time-periodic external magnetic field, $b(t)$, may be varied over a wide range: typical values are $b_0 \sim 0.01$–10^2 Oe. A typical cavity quality factor is $Q \sim 10^4$, or even higher [17]. (Here $Q = \omega/2\gamma$ and γ is the damping coefficient of our eigenmode.) The dynamics may be taken to be nondissipative over times t less than order $10^4/\omega$. The feasibility of making experimental measurements of effects connected with time scale $\tau_{\hbar}$ less than this will be discussed below.

The eigenmodes $\boldsymbol{E}_k(\boldsymbol{r})$ in the ideal cavity resonator are described by the Helmholtz equation,

$$\Delta \boldsymbol{E}_k + \left(\frac{\omega_k}{c}\right)^2 \boldsymbol{E}_k = \boldsymbol{0} , \quad \nabla \cdot \boldsymbol{E}_k = 0, \tag{2.1}$$

with tangential boundary conditions $\boldsymbol{E}_k \times \boldsymbol{n} = \boldsymbol{0}$ (where $\boldsymbol{n}$ is a normal vector to the resonator surface). The magnetic field $\boldsymbol{B}_k(\boldsymbol{r})$ also satisfies eqs. (2.1) but with normal boundary conditions, $\boldsymbol{B}_k \cdot \boldsymbol{n} = 0$. The eigenfrequencies depend on the shape of the resonator, and for a rectangular parallelepiped with sides L_x, L_y, L_z, one has

$$\left(\frac{\omega_k}{c}\right)^2 = k_x^2 + k_y^2 + k_z^2 , \tag{2.2}$$

where

$$k_{x,y,z} = n_{x,y,z}/L_{x,y,z} ,$$

and $n_{x,y,z} = 0, 1, \ldots$.

For quantum considerations the electromagnetic field in the resonator may be represented in the well-known form

$$\boldsymbol{E}(\boldsymbol{r}, t) = \sum_k \hat{p}_k(t) \boldsymbol{E}_k(\boldsymbol{r}) ,$$

$$\boldsymbol{B}(\boldsymbol{r}, t) = -\sum_k \omega_k \hat{q}_k(t) \boldsymbol{B}_k(\boldsymbol{r}) , \tag{2.3}$$

where $\hat{p}_k(t)$ and $\hat{q}_k(t)$ are impulse and coordinate operators, with commutation relations $[\hat{q}_k, \hat{p}_{k'}] = i\hbar\delta_{k,k'}$. The operators $\hat{q}_k$ and $\hat{p}_k$ are expressible in terms of creation and annihilation operators $\hat{a}^+$ and $\hat{a}$, as

$$\hat{q}_k = \left(\frac{\hbar}{2\omega_k}\right)^{1/2} (\hat{a}_k^+ + \hat{a}_k) ,$$

$$\hat{p}_k = i(\tfrac{1}{2}\hbar\omega_k)^{1/2} (\hat{a}_k^+ - \hat{a}_k) , \tag{2.4}$$

with commutator $[\hat{a}_k, \hat{a}_{k'}^+] = \delta_{k,k'}$. Hence, we arrive at the standard formula for the Hamiltonian of an electromagnetic field in a resonator,

$$\hat{H}_0 = \frac{1}{8\pi} \int (\boldsymbol{B}^2 + \boldsymbol{E}^2) \, dV$$

$$= \sum_k \hbar\omega_k (\hat{a}_k^+ \hat{a}_k + \tfrac{1}{2}) . \tag{2.5}$$

The interaction of N spins in a sample placed in this resonator with a magnetic field is governed by the Hamiltonian

$$\hat{H}_{\text{int}} = g\mu_B [\boldsymbol{B}(\boldsymbol{r}_0, t) + \boldsymbol{B}_{\text{ex}}] \cdot \sum_{j=1}^{N} \hat{\boldsymbol{S}}_j . \tag{2.6}$$

In (2.6) $\boldsymbol{B}_{\text{ex}}$ is an external magnetic field that is as-

sumed to be homogeneous over the sample's size and could depend on time; $\hat{S}_j$ are spin operators; N is the number of spins in the example. We have substituted $\boldsymbol{B}(\boldsymbol{r}_0, t)$ for $\boldsymbol{B}(\boldsymbol{r}, t)$ in (2.6), with

$$\boldsymbol{B}(\boldsymbol{r}_0, t) = -\sum_{\boldsymbol{k}} (\tfrac{1}{2}\hbar\omega_{\boldsymbol{k}})^{1/2} \boldsymbol{B}_{\boldsymbol{k}}(\boldsymbol{r}_0)(\hat{a}_{\boldsymbol{k}}^{+} + \hat{a}_{\boldsymbol{k}}) , \quad (2.7)$$

since the size of the sample being placed into the resonator near location $\boldsymbol{r} \approx \boldsymbol{r}_0$ is supposed to be small in comparison with the characteristic inhomogeneity of the chosen resonator eigenmode. The magnetic field in such a sample may be regarded as homogeneous. In what follows, we shall limit ourselves to the single-mode approximation and consider the following eigenmode of the resonator,

$$E_z(x, y) = \sqrt{16\pi/V} \sin(k_x x) \sin(k_y y) ,$$

$$E_x = E_y = 0 ,$$

$$B_x(x, y) = -\frac{ck_y}{\omega} \sqrt{16\pi/V} \sin(k_x x) \cos(k_y y) ,$$

$$B_y(x, y) = \frac{ck_x}{\omega} \sqrt{16\pi/V} \cos(k_x x) \sin(k_y y) ,$$

$$B_z = 0 , \quad (2.8)$$

where

$$k_{x,y} = \pi/L_{x,y} , \quad V = L_x L_y L_z ,$$

$$\omega^2 = c^2(k_x^2 + k_y^2) . \quad (2.9)$$

The normalization of the mode is chosen as

$$\int \boldsymbol{E}^2 \, \mathrm{d}V = \int \boldsymbol{B}^2 \, \mathrm{d}V = 4\pi .$$

According to (2.8) the electromagnetic field is homogeneous along the z axis. Thus, it is sufficient to assume that the dimensions of the sample along the x and y axes are small,

$$l_x \ll L_x , \quad l_y \ll L_y . \quad (2.10)$$

For example, we could satisfy these conditions by placing our sample in the resonator near $x = \frac{1}{2}L_x$, $y = 0$. This corresponds to putting the sample at the location of the maximum of the magnetic field, where it is polarized along the x axis (see fig. 1). Next, we assume that the spatially homogeneous magnetic field $\boldsymbol{B}_{\mathrm{ex}}$ in (2.6) includes a constant component, $\boldsymbol{B}_0$, directed along the z axis, as well as a time-periodic component, directed along the x axis and given by

$$b(t) = b_0 \cos(\Omega t) . \quad (2.11)$$

Thus, b_0 and Ω denote the amplitude and frequency of the time-periodic component of the homogeneous external magnetic field. We also assume that the following frequency conditions are satisfied,

$$\gamma < |\omega - \Omega| \ll \omega, \Omega . \quad (2.12)$$

We shall discuss experimental parameters corresponding to this condition in the conclusion.

Now writing (2.5) and (2.6) with only one mode (2.8) yields the following Hamiltonian for our system,

$$\hat{H} = \hbar\omega \hat{a}^{+}\hat{a} + g\mu_{\mathrm{B}} B_0 \sum_{j=1}^{N} \hat{S}_j^z + \frac{g\mu_{\mathrm{B}} c k_y}{\omega} \sqrt{\frac{2\pi\hbar\omega}{V}} \sum_{j=1}^{N} (\hat{S}_j^{+} + \hat{S}_j^{-})(\hat{a}^{+} + \hat{a}) + \tfrac{1}{2} g\mu_{\mathrm{B}} b_0 \cos(\Omega t) \sum_{j=1}^{N} (\hat{S}_j^{+} + \hat{S}_j^{-}) . \quad (2.13)$$

Below, we show that the strength of interaction between the spins and the resonator mode is determined by the real-valued coupling constant

$$\Lambda_0 = \sqrt{\frac{2\pi c^2 k_y^2 \mu_{\mathrm{B}}^2 g^2 N}{\hbar\omega^3 V}} . \quad (2.14)$$

The quantum effects in which we are interested depend significantly on the number of spins, N. Thus, it is convenient to introduce experimentally controllable parameters that allow us to vary the number of spins, N, at a fixed value of the coupling, Λ_0. For this purpose, we choose the linear dimensions of the sample to satisfy

$$l_{x,y} \ll L_{x,y} , \quad l_z = L_z . \quad (2.15)$$

In this case, the field $B_x(x, y)$ in (2.8) may be considered as homogeneous over the size of the sample. The number of spins in the sample is: $N = \rho_0 l_x l_y l_z$ (where ρ_0 is the density of spins); so the constant Λ_0 does not depend on L_z, since by (2.14)

$$\Lambda_0 = \sqrt{\frac{2\pi c^2 k_y^2 \mu_{\mathrm{B}}^2 g^2 l_x l_y \rho_0}{\hbar\omega^3 L_x L_y}} . \quad (2.16)$$

At the same time, N is proportional to L_z, so N may be varied at constant Λ_0. Estimates of these param-

eters will be discussed in the conclusion.

3. Slow dynamics and time-independent Hamiltonian

In this section we simplify Hamiltonian (2.13). For this, we use the interaction representation $\Psi_{\rm int}=\exp(i\hat{H}_0 t/\hbar)\Psi$ with Hamiltonian operator $\hat{H}_0$ given by

$$\hat{H}_0=\hbar\omega\hat{a}^+\hat{a}+g\mu_B B_0\sum_{j=1}^{N}\hat{S}_j^z\,, \tag{3.1}$$

and introduce "collective operators"

$$\hat{A}=\hat{a}/\sqrt{N}\,,\quad \hat{A}^+=\hat{a}^+/\sqrt{N}\,,$$

$$\hat{S}^{\pm,z}=\frac{1}{N}\sum_{j=1}^{N}\hat{S}_j^{\pm,z}\,. \tag{3.2}$$

These collective operators satisfy the following renormalized commutation relations,

$$[\hat{A},\hat{A}^+]=\frac{1}{N}\,,\quad [\hat{S}^{\pm},\hat{S}^z]=\pm\frac{1}{N}\hat{S}^{\pm}\,,$$

$$[\hat{S}^+,\hat{S}^-]=\frac{2}{N}\hat{S}^z\,, \tag{3.3}$$

where $\hat{S}^{\pm}=\hat{S}^x\pm i\hat{S}^y$. In the interaction representation, using (2.13) leads to the following Hamiltonian for the slow dynamics of the system (dropping nonresonant terms),

$$\hat{\tilde{H}}_{\rm int}(\tau)=N[(\hat{A}\hat{S}^+ +\hat{A}^+\hat{S}^-)$$
$$+\lambda(e^{i\bar{\Delta}\tau}\hat{S}^- +e^{-i\bar{\Delta}\tau}\hat{S}^+)]\,,$$

$$i\frac{\partial\tilde{\Psi}_{\rm int}(\tau)}{\partial\tau}=\hat{\tilde{H}}_{\rm int}(\tau)\tilde{\Psi}_{\rm int}(\tau)\,. \tag{3.4}$$

In (3.4) a slow dimensionless time, $\tau=\omega_c t$, and a dimensionless constant of interaction of paramagnetic atoms with the external field have been introduced, where

$$\lambda=\frac{g\mu_B b_0}{4\hbar\omega\Lambda_0}\,,\quad \omega_c=\omega\Lambda_0\,,\quad \bar{\Delta}=(\Omega-\omega)/\omega_c\,. \tag{3.5}$$

The wave function $\tilde{\Psi}_{\rm int}(\tau)$ describes the slow dynamics of our system in the interaction representation. In deriving Hamiltonian (3.4) we have assumed that $\Lambda_0\ll 1$, which allows the dynamics of the system to be separated into slow and fast motion. When the condition $\Lambda_0\ll 1$ is satisfied, one may neglect the fast terms in the Hamiltonian ($\sim\exp(\pm 2i\omega t)$) and use the rotating wave approximation (RWA). So, in this case we have: $\omega_c/\omega\sim\Lambda_0\ll 1$. The slow frequency ω_c introduced in (3.5) plays here the role of a "cooperative frequency", that characterises the time scale for energy exchange between paramagnetic atoms and the self-consistent field in the resonator.

The canonical change of variables

$$\hat{\eta}^+=e^{-i\bar{\Delta}\tau}\hat{S}^+\,,\quad \hat{\eta}^z=\hat{S}^z\,,\quad \hat{c}=e^{i\bar{\Delta}\tau}\hat{A}\,, \tag{3.6}$$

makes the Hamiltonian time-independent (cf. eq. (3.4)),

$$\hat{H}=N(\hat{c}\hat{\eta}^+ +\hat{c}^+\hat{\eta}^- +\lambda\hat{\eta}^+ +\lambda\hat{\eta}^-$$
$$-\bar{\Delta}\hat{c}^+\hat{c}-\bar{\Delta}\hat{\eta}^z)\,. \tag{3.7}$$

The equations resulting from this Hamiltonian possess in general only two integrals of motion: $\hat{H}$ in (3.7) and $\hat{S}^2$, given by

$$\hat{S}^2=(\hat{\eta}^z)^2+\tfrac{1}{2}(\hat{\eta}^+\hat{\eta}^- +\hat{\eta}^-\hat{\eta}^+)\,. \tag{3.8}$$

However, when $\lambda=0$, a third integral of motion exists,

$$\hat{W}=\hat{c}^+\hat{c}+\hat{\eta}^z\,, \tag{3.9}$$

and the problem becomes completely integrable.

In fact, the problem formulated so far is identical to the well-known quantum Dicke model (QDM) (see, for example, reviews [16,17] and references therein). QDM is a completely integrable system, and more than twenty years ago numerical results for this model were obtained [15] that foreshadow how the time scale $\tau_\hbar\sim\ln N$ for violation of the semi-classical approximation arises in the system governed by Hamiltonian (3.4).

The authors of ref. [15] numerically compute the quantum dynamics and corresponding classical motion in QDM, starting from an initial "super radiant" state, and from an initially completely inverted state (CIS). For CIS, they find that the quantum slow dynamics and its corresponding classical limit first begin to differ on a time scale $\tau_\hbar\sim\ln N$. The conclusion in the present paper is the following: if in the semi-classical approximation, there exists developed chaos (global instability over most of phase space), then the time scale $\tau_\hbar\sim\ln N$ will be the

characteristic time, after which significant differences may arise between the classical and quantum dynamics. Roughly speaking, one can say that the logarithm appears in $\tau_{\hbar}$ because of local exponential instability of classical trajectories in phase space, and N appears because N is the only "quantum" parameter appearing in Hamiltonian (3.4) and commutation relations (3.3).

4. Exact c-number equations for quantum expectation values

In this section, we use a method suggested in refs. [18–20] for deriving closed c-number PDEs that govern the dynamics of quantum expectation values in boson and spin coherent states [21] at $\tau=0$,

$$|z\rangle=\exp(Nz\hat{A}^{+}-Nz^{*}\hat{A})|0\rangle\,, \tag{4.1}$$

where

$$\hat{A}|z\rangle=z|z\rangle\,, \tag{4.2}$$

and the average number of photons in the resonator mode at $\tau=0$ is

$$n(0)\equiv\langle z|\hat{a}^{+}\hat{a}|z\rangle=N\langle z|\hat{A}^{+}\hat{A}|z\rangle$$
$$=N|z|^{2}\,. \tag{4.3}$$

We also introduce spin coherent states [22] at $\tau=0$,

$$|\xi\rangle=(1+|\xi|^{2})^{-J}\exp(\xi\hat{J}^{+})|J,-J\rangle\,, \tag{4.4}$$

where

$$\hat{J}=\sum_{j=1}^{N}\hat{S}_{j}=N\hat{S}\,,$$

$$\hat{J}^{2}|J,M\rangle=J(J+1)|J,M\rangle\quad(M=-J,...,J)\,,$$

$$J=0,\tfrac{1}{2},...,\tfrac{1}{2}N,\quad|z|,|\xi|\in[0,\infty)\,. \tag{4.5}$$

Now, the time-dependent expectation value at time τ of an arbitrary Heisenberg operator $\hat{f}(\tau)$ is given by

$$f(\tau)=\langle\xi,z|\hat{f}(\tau)|z,\xi\rangle\,, \tag{4.6}$$

where $|z,\xi\rangle=|z\rangle|\xi\rangle$. Using the method discussed in refs. [18,19] (see also ref. [20]) gives the following equation for expectation value $f(\tau)$ in (4.6),

$$\frac{\partial f(\tau)}{\partial\tau}=\hat{\mathscr{K}}f(\tau)\,,\quad f(0)=f(z,z^{*};\xi,\xi^{*})\,, \tag{4.7}$$

where the differential operator $\hat{\mathscr{K}}$ separates additively into its classical and quantum contributions, as

$$\hat{\mathscr{K}}=\hat{\mathscr{K}}_{\mathrm{cl}}+\frac{1}{N}\hat{\mathscr{K}}_{\mathrm{q}}\,, \tag{4.8}$$

with

$$\hat{\mathscr{K}}_{\mathrm{cl}}=\mathrm{i}\Big[-\bar{\Delta}z^{*}\frac{\partial}{\partial z^{*}}+\bar{\Delta}z\frac{\partial}{\partial z}-\bar{\Delta}\xi^{*}\frac{\partial}{\partial\xi^{*}}+\bar{\Delta}\xi\frac{\partial}{\partial\xi}$$
$$+\frac{2J}{N}\frac{1}{1+|\xi|^{2}}\Big(\xi^{*}\frac{\partial}{\partial z^{*}}-\xi\frac{\partial}{\partial z}\Big)$$
$$+\Big(z^{*}\frac{\partial}{\partial\xi^{*}}-z\frac{\partial}{\partial\xi}\Big)+\Big(z^{*}\xi^{2}\frac{\partial}{\partial\xi}-z\xi^{*}\frac{\partial}{\partial\xi^{*}}\Big)$$
$$+\lambda\Big(\frac{\partial}{\partial\xi^{*}}-\frac{\partial}{\partial\xi}+\xi^{2}\frac{\partial}{\partial\xi}-\xi^{*2}\frac{\partial}{\partial\xi^{*}}\Big)\Big]\,, \tag{4.9}$$

and

$$\hat{\mathscr{K}}_{\mathrm{q}}=\mathrm{i}\Big(\xi^{2}\frac{\partial^{2}}{\partial z\partial\xi}-\xi^{*2}\frac{\partial^{2}}{\partial z^{*}\partial\xi^{*}}\Big)\,. \tag{4.10}$$

The semi-classical approximation corresponds to the following limit,

$$N\to\infty\,,\quad J\to\infty\,,\quad\sigma=2J/N\to\text{const.} \tag{4.11}$$

5. Classical limit

In the classical limit we have from (4.7) and (4.8) for $f(\tau)$

$$\frac{\partial f(\tau)}{\partial\tau}=\hat{\mathscr{K}}_{\mathrm{cl}}f(\tau)\,. \tag{5.1}$$

Since the operator $\hat{\mathscr{K}}_{\mathrm{cl}}$ in (4.9) involves only first-order derivatives, the classical solution may be obtained by the method of characteristics. Using the explicit form of the operator $\hat{\mathscr{K}}_{\mathrm{cl}}$ in (4.9) leads to characteristic equations,

$$\frac{\mathrm{d}z}{\mathrm{d}\tau}=\mathrm{i}\bar{\Delta}z-\mathrm{i}\frac{\sigma\xi}{1+|\xi|^{2}}\,,\quad\sigma=\frac{2J}{N}\,,$$

$$\frac{\mathrm{d}\xi}{\mathrm{d}\tau}=\mathrm{i}\bar{\Delta}\xi-\mathrm{i}z+\mathrm{i}z^{*}\xi^{2}-\mathrm{i}\lambda+\mathrm{i}\lambda\xi^{2}\,. \tag{5.2}$$

The solutions of eqs. (5.2) determine the time-

dependence of any semi-classical function, for example

$$S^+(\tau)=\frac{\sigma\xi^*(\tau)}{1+|\xi(\tau)|^2},$$

$$S^z(\tau)=-\frac{\sigma(1-|\xi(\tau)|^2)}{2(1+|\xi(\tau)|^2)},\quad A(\tau)=z(\tau). \qquad (5.3)$$

Figure 2 shows the Poincaré map of a semi-classical trajectory obtained from (5.2) and displayed on the plane $x=\mathrm{Re}(z)$, $y=\mathrm{Im}(z)$ at the moments when the trajectory crosses the plane $\mathrm{Re}\,\xi(\tau)=0$. We note also that the semi-classical dynamics can be described by the Hamiltonian

$$H_{\mathrm{cl}}=\bar{\Delta}(q^2+p^2-x^2-y^2)$$
$$+2(\sigma-q^2-p^2)^{1/2}(xq-yp+\lambda q)$$
$$=E, \qquad (5.4)$$

where the following canonical variables are introduced (with $\sigma=2J/N=\mathrm{const}$),

$$z=x+\mathrm{i}y,\quad \zeta\equiv\frac{\sqrt{\sigma}\,|\xi|}{\xi\sqrt{1+|\xi|^2}}=q+\mathrm{i}p, \qquad (5.5)$$

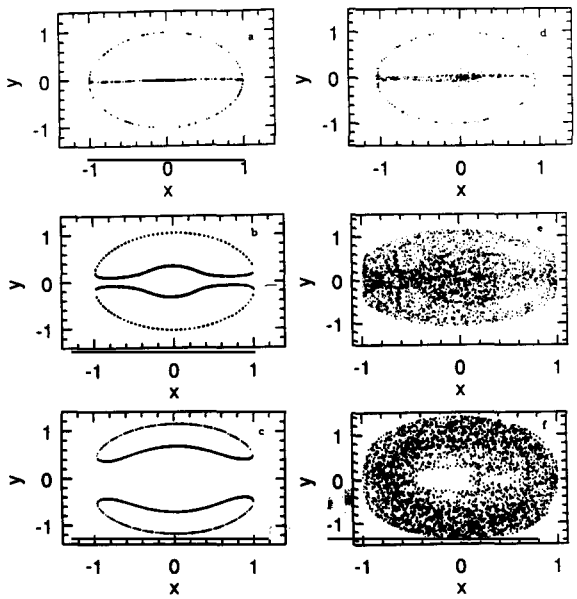

Fig. 2. The Poincaré map of a semi-classical trajectory on the plane (x, y) ($\sigma=1$, $\bar{\Delta}=1$). Integrable cases ($\lambda=0$): (a) separatrix with $E=0$, $W=0$; (b) $E=0$, $W=0.1$; (c) $E=0$, $W=0.4$. Nonintegrable cases ($\lambda\neq 0$): (d) $\lambda=10^{-3}$, $E=0$; (e) $\lambda=0.1$, $E=0$; (f) $\lambda=2$, $E=0$.

with canonically conjugated pairs (x, y) and (q, p), and rescaled time $\tau'=2\tau$.

As we already mentioned, the case $\lambda=0$ is completely integrable, and the third integral has the form

$$W=\langle\hat{W}\rangle=x^2+y^2-q^2-p^2. \qquad (5.6)$$

Curve (a) in fig. 2 corresponds to the separatrix ($E=0$, $W=0$), given on the plane (x, y) as

$$x^2+y^2=\sigma,\quad y\neq 0\quad(\lambda=0),$$
$$x\in[-\sqrt{\sigma},\sqrt{\sigma}],\quad y=0. \qquad (5.7)$$

Curves (b) and (c) in fig. 2 correspond to the integrable case, but with $W\neq 0$. Curves (d), (e), (f) show the transition to developed (global) chaos, as the dimensionless coupling constant λ increases. Our numerical calculations show that a qualitative criterion for developed semi-classical chaos to occur in the system may be expressed as

$$\lambda\sim\bar{\Delta}\sim 1, \qquad (5.8)$$

or, in dimensional form,

$$\omega_{\mathrm{c}}\sim\omega_{\mathrm{R}}\sim|\Delta|,$$

where $\omega_{\mathrm{c}}=\omega\Lambda_0$ is the cooperative frequency; $\omega_{\mathrm{R}}=g\mu_{\mathrm{B}}b_0/2\hbar$ is the Rabi frequency and $\Delta=\Omega-\omega$ is the detuning.

The semi-classical version of model (3.4) is studied in refs. [23–25], in connection with a problem in nonlinear optics that is mathematically identical to the problem considered in this paper. In ref. [23] global semi-classical chaos for this problem is investigated numerically. In ref. [24,25] exact results are derived for the case of weak (homoclinic) chaos for $\lambda\ll 1$ in the semi-classical case. Figure 3 shows time series for the case of developed semi-classical chaos. These numerical calculations show that the dynamics in this case is locally unstable. Thus, one could expect considerable influence of quantum corrections on this semi-classical dynamics. We turn to this issue in the next section.

6. The influence of quantum corrections on chaotic semi-classical motion

The quantum correlation function for two arbitrary operators $\hat{f}(\tau)$ and $\hat{g}(\tau)$ is defined to be

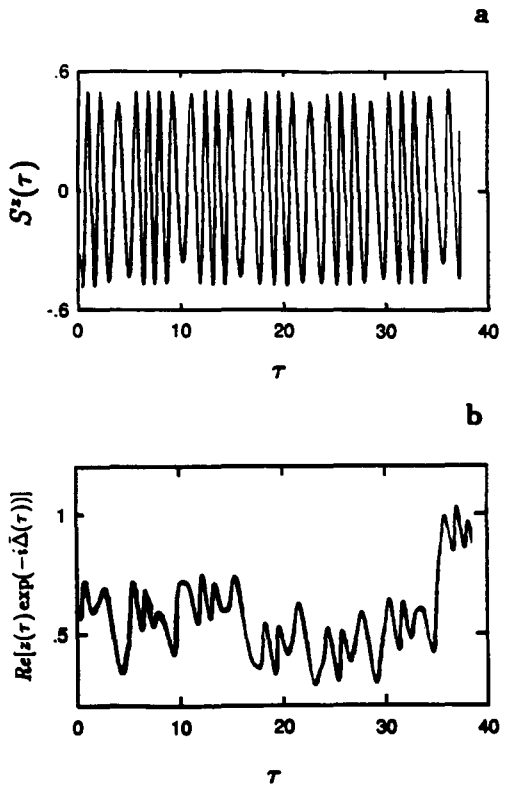

Fig. 3. Chaotic dynamics in the semi-classical approximation: (a) time-dependence $S^z(\tau)$; (b) time-dependence $\mathrm{Re}[z(\tau)\times\exp(-i\bar{\Delta}\tau)]$; $\bar{\Delta}=1$, $\sigma=1$, $\lambda=2$, $z(0)\approx(0.65;\ -0.34)$, $\xi(0)\approx(0;-1.75)$.

$$\frac{1}{N}P_{f,g}(\tau)=\langle\xi,z|\hat{f}(\tau)\hat{g}(\tau)|z,\xi\rangle - \langle\xi,z|\hat{f}(\tau)|z,\xi\rangle\langle\xi,z|\hat{g}(\tau)|z,\xi\rangle\,. \tag{6.1}$$

To derive the quantum correlation function dynamics for $P_{f,g}(\tau)$, we note that all three terms in (6.1) satisfy eq. (4.7). Taking this into account gives an *exact* equation for $P_{f,g}(\tau)$,

$$\frac{\partial P_{f,g}}{\partial\tau}=\hat{\mathcal{K}}_{\mathrm{cl}}P_{f,g}-i\xi^{*2}\left(\frac{\partial f}{\partial z^*}\frac{\partial g}{\partial\xi^*}+\frac{\partial g}{\partial z^*}\frac{\partial f}{\partial\xi^*}\right) +i\xi^{2}\left(\frac{\partial f}{\partial z}\frac{\partial g}{\partial\xi}+\frac{\partial g}{\partial z}\frac{\partial f}{\partial\xi}\right)+\frac{1}{N}\hat{\mathcal{K}}_{\mathrm{q}}P_{f,g}\,, \tag{6.2}$$

where the operators $\hat{\mathcal{K}}_{\mathrm{cl}}$ and $\hat{\mathcal{K}}_{\mathrm{q}}$ are given in (4.9) and (4.10), and we denote

$$f\equiv\langle\xi,z|\hat{f}(\tau)|z,\xi\rangle\,,\quad g\equiv\langle\xi,z|\hat{g}(\tau)|z,\xi\rangle\,. \tag{6.3}$$

Using the correlation functions (6.1) and the Heisenberg equations for the operators: $\hat{c}^+$, $\hat{c}$, $\hat{\eta}^z$, $\hat{\eta}^+$, $\hat{\eta}^-$ gives a set of exact c-number equations for their expectation values, namely,

$$\dot{c}=i\bar{\Delta}c-i\eta^-\,,\quad \dot{\eta}^-=i\bar{\Delta}\eta^-+2i\lambda\eta^z+2i\eta^z c+\frac{2i}{N}P_{\eta^z,c}\,,$$

$$\dot{\eta}^z=ic^+\eta^- -ic\eta^+ +i\lambda\eta^- -i\lambda\eta^+ +\frac{i}{N}(P_{c^+,\eta^-}-\mathrm{c.c.})\,. \tag{6.4}$$

In (6.4) c^+, c, η^z, η^+, η^- are c-number functions defined according to (6.3). Equations (6.2) and (6.4) form a closed set of c-number equations which describes the quantum dynamics of expectation values and quantum correlation functions.

It was already mentioned above that the only quantum parameter appearing in our system is $\epsilon=1/N$. The physical meaning of this parameter is rather simple. Since Hamiltonian (3.4) (or (3.7)) is expressed in collective variables, the characteristic action in the system, I, is proportional to the number of atoms N and the quasiclassical parameter is of the order $\kappa=I/\hbar\sim N$. In this connection, we note that the problem considered here is directly related to the well known $1/N$ expansion (see, for example, review [26]).

It is clear from (6.1) that quantum correlations may be significant for small enough N. Here we are mainly interested in the case that N is large enough that one may expect (at least for finite times $\tau<\tau_{\hbar}$) semi-classical chaotic dynamics to appear. In this case, numerical investigation of eqs. (6.2) and (6.4) may be accomplished by using a rather simple scheme, connected with the $1/N$ expansion. Not unexpectedly, this method usually leads to secular growth connected with the presence of small parameters multiplying the highest-derivative terms in (6.2). We study numerically the secular effect of these quantum corrections on the semi-classical solution over finite times. The accuracy of this approach can be checked by verifying conservation of the quantum integrals of motion, $\langle\hat{H}\rangle$, $\langle\hat{S}^2\rangle$, and $\langle\hat{W}\rangle$, when $\lambda=0$. In this approach, the first step in constructing a solution for $N\gg1$ consists of neglecting in (6.4) all quantum correlations and constructing a semi-classical solution (as in section 5). Then,

substituting this solution instead of functions f and g into (6.2) and neglecting the last term allows us to calculate approximate quantum correlation functions, $P_{fg}(\tau)$. The last step in constructing an approximate quantum solution consists of calculating quantum expectation values in (6.4), taking into account quantum correlation functions. Numerical results obtained using this scheme are presented in figs. 4–7. In fig. 4 the characteristic dependence of the time scale $\tau_\hbar$ for departure from the semi-classical solution because of quantum correlations is shown as a function of $\ln N$ for several parameter values. (This dependence of $\tau_\hbar(N)$ is given in fig. 4 under the condition of developed chaos in the semi-classical approximation.) In fig. 5 the analogous behavior of $\tau_\hbar$ is shown as a function of N. The results presented in figs. 4 and 5 show that in the case of developed chaotic dynamics in the semi-classical limit the dependence $\tau_\hbar(N)$ is logarithmic. In the last case, the time scale $\tau_\hbar$ is found by numerical experiment following ref. [20], by using the so-called "1% criterion". Namely, a quantum solution is calculated according to the $1/N$ scheme explained above and a quantum vector function $\boldsymbol{D}(\tau)=(c(\tau),\ \eta^+(\tau),\ \eta^z(\tau),)$ and its semi-classical analog $\boldsymbol{D}_{\rm cl}(\tau)$ are found. Then, we calculate the function

$$\delta(\tau)=[\,|c_{\rm cl}(\tau)|+|\eta^+_{\rm cl}(\tau)|+|\eta^z_{\rm cl}(\tau)|\,]^{-1}\times|c(\tau)-c_{\rm cl}(\tau)|+|\eta^+(\tau)-\eta^+_{\rm cl}(\tau)|+|\eta^z(\tau)-\eta^z_{\rm cl}(\tau)|\,, \tag{6.5}$$

which describes the relative difference between quantum and semi-classical solutions. The time scale $\tau_\hbar(N)$ is obtained by setting $\delta(\tau_\hbar)=\text{const}=10^{-2}$, with $\delta(0)=0$. The number of atoms N is varied according to the law: $N=2^n$ ($n=2$, ..., 30). So, $N_{\max}$ has the value $N_{\max}\sim 10^9$. Figure 6 shows the dependence of $\tau_\hbar$ on N for regular dynamics in the semi-classical approximation calculated according to the "1% criterion" for $\lambda=0.1$, $E=0$, $W(0)=0.3$, $\sigma=1$, $\bar{\Delta}=1$. Finally, fig. 7 shows numerical results for the time-dependence of the quantum correlation function,

$$P(\tau)=|P_{c+,c}(\tau)|+|P_{Sz,c}(\tau)|+|P_{c+,S-}(\tau)|\,. \tag{6.6}$$

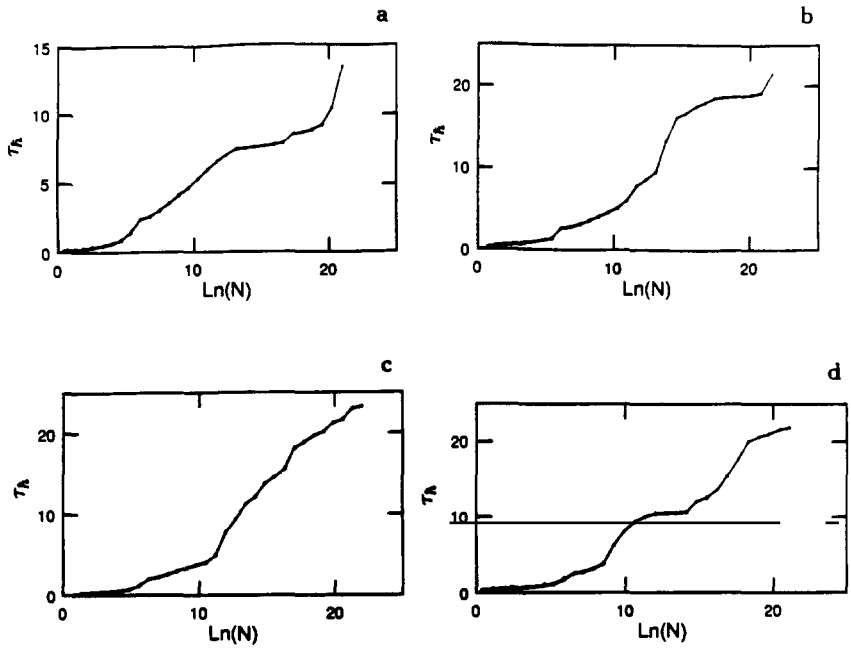

Fig. 4. Dependence $\tau_\hbar(N)$ on $\ln N$ for developed chaotic dynamics in the semi-classical approximation calculated according to the "1% criterion"; $\bar{\Delta}=1$, $\sigma=1$; (a) $E=0$, $\lambda=0.2$, $W(0)=0.3$; (b) $E=0$, $\lambda=0.3$, $W(0)=0.3$; (c) $E=0$, $\lambda=0.5$, $W(0)=0.3$; (d) $E=0.1$, $\lambda=0.5$, $W(0)=0.1$.

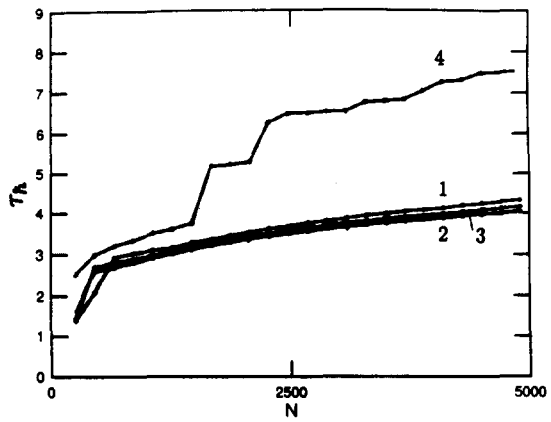

Fig. 5. Dependence $\tau_h(N)$ for developed chaotic dynamics in the semi-classical approximation; $E=0$, $W(0)=0.3$, $\sigma=1$, $\bar{A}=1$; (1) $\lambda=0.1$; (2) $\lambda=0.2$; (3) $\lambda=0.3$; (4) $\lambda=2$ ("1% criterion" was used).

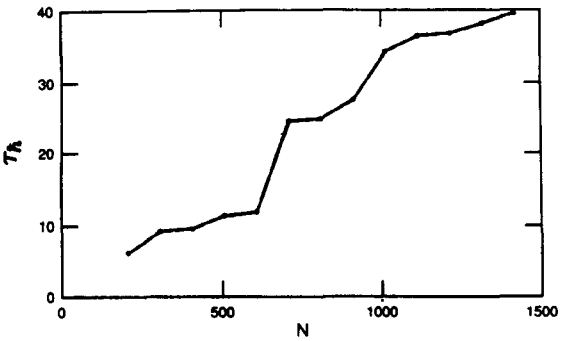

Fig. 6. Dependence $\tau_h(N)$ for regular dynamics in the semi-classical approximation calculated according to the "1% criterion"; $\lambda=0.1$, $E=0$, $W(0)=0.3$, $\sigma=1$, $\bar{A}=1$.

The function $P(\tau)$ is shown in fig. 7a for the case of developed semi-classical chaos, and in fig. 7b for the case of regular semi-classical dynamics. As one can see from fig. 7, when the semi-classical approximation exhibits developed chaos, the quantum correlation function $P(\tau)$ grows exponentially. When the semi-classical dynamics is regular, the quantum correlation function $P(\tau)$ grows significantly slower, roughly as an algebraic power law. Of course, in the semi-classical approximation $P^{(sc)}(\tau)$ remains zero. The dependence of $P(\tau)$ shown in fig. 7 is typical;

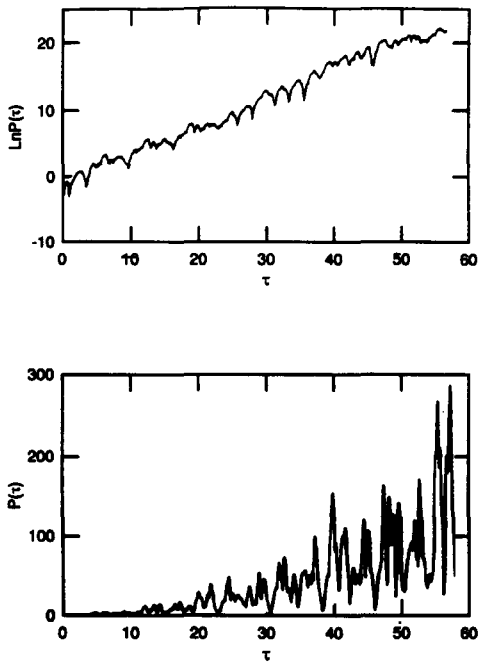

Fig. 7. Time-dependence of quantum correlation function $P(\tau)$; (a) the case of developed chaos in the semi-classical limit: $\bar{A}=1$, $\sigma=1$, $\lambda=1$; (b) the case of regular semi-classical dynamics: $\bar{A}=3$, $\sigma=1$, $\lambda=1$.

the same form also appears for other quantum correlation functions.

7. Conclusion

Materials with strong concentrations of free radicals may be suitable for experimental observation of the quantum effects we discuss here, arising in transition from nondissipative semiclassical dynamics [27–29]. In the solid state, these materials have rather thin PMR lines, and the value of the g-factor is close to 2. One of the best known of such materials has chemical composition: α,α-diphenyl-B-picryl hydrazyl (DPPH). This material is used as a standard for PMR and has a half-width at half-height $\frac{1}{2}\Delta B \sim 1$ Oe. The value ΔB depends weakly on temperature, and on the frequency at which the measurement is made. For example, if we use as a solvent from which a sample of DPPH is crystallized, then we have

$\frac{1}{2}\Delta B = 1.45$ Oe, for $f = 300$ MHz, $T = 295$ K,
$\frac{1}{2}\Delta B = 1.3$ Oe, for $f = 9.4$ GHz, $T = 295$ K,
$\frac{1}{2}\Delta B = 1.3$ Oe, for $f = 300$ MHz, $T = 90$ K. (7.1)

The average distance between unpaired electrons in DPPH $\sim 10^{-7}$ cm corresponds to the density $\rho_0 = 10^{21}$ cm^{-3}. The thin width and large density guarantee a high level of PMR signal, allowing measurements with as little as $\sim 10^{-9}$ g of DPPH. Note, that in experiments even thinner PMR lines were observed. For example, DPPH in a solution of carbon bisulphide has $\frac{1}{2}\Delta B = 0.65$ Oe; and Picryl-n-amino-car-bazyl [28] (whose structure is slightly different from DPPH), has $\frac{1}{2}\Delta B = 0.25$ Oe which corresponds to $\frac{1}{2}\Delta f = 70$ kHz.

Now we give numerical estimates for the interaction constants Λ_0 and λ corresponding to a typical PMR frequency $f = 1$ GHz and $\rho_0 = 10^{21}$ cm^{-3}. Assume $k_y^2 \gg k_x^2$, then approximately $\omega^2 \approx c^2 k_y^2$ and $L_y \approx 15$ cm. Let us put $L_x \approx 40$ cm, then substituting these values into (2.16) and assuming $l_y = 3$ cm, $l_x = 6$ cm gives

$$\Lambda_0 \approx 0.1 . \tag{7.2}$$

Varying L_z, for example, from $L_z = 0.4$ cm up to $L_z = 40$ cm one could vary N from 7×10^{21} cm^{-3} up to 7×10^{23} cm^{-3}. The value Λ_0 remains constant for these variations. We estimate now the dimensionless value of λ for the parameter values chosen above. From (3.5) we have

$$\lambda \approx 10^{-2} b_0 \,(\text{Oe}) . \tag{7.3}$$

So, as b_0 varies in the range $b_0 = 10^{-3}$–10^2 Oe, the value λ varies in the range $\lambda = 10^{-5}$–1. Finally, for the cooperative frequency in this case we have $\omega_c = 2\pi f \Lambda_0 \approx 0.63$ GHz. With these parameter values, the conditions for developed semi-classical chaos are $b_0 \approx 10^2$ Oe, $\Delta \approx \omega_c$.

We envision the following experimental setup: In the resonator an electromagnetic wave is injected with nonresonant frequency Ω. After a time interval $\tau > Q/\pi f$ in the resonator, oscillations with frequency Ω will be established. The frequency Ω differs from the resonant frequency ω of spins, so the influence of the external field on the spin system is small. At the time moment $t_0 > Q/\pi f$ the electron magnetization is inclined from the z axis. After this, for times

$$\Delta t \sim \min\{Q/\pi f, (\pi \Delta f)^{-1}\} \tag{7.4}$$

a dynamical process will be realized which corresponds to Hamiltonian (3.7). We have also assumed that temperature effects are small ($\hbar\omega > T$). Unfortunately, this leads to rather strict limitations on the temperature: at $f = 10^9$ GHz the temperature should be $T < 10^{-1}$ K.

So far, the choice of parameters has been restricted to keep the constant Λ_0 in (2.16) sufficiently large ($\Lambda_0 \approx 0.1$). Relaxing this restriction allows the possibility of increasing the resonant frequency ω. So the dimension of the resonator and of the sample could be reduced and the allowed temperature could be increased. The decrease of Λ_0 in this case would not preclude observation of quantum effects that violate the semi-classical approximation.

Acknowledgement

Two of the authors (G.P.B. and E.N.B.) would like to thank G. Doolen and J.M. Hyman of the Center for Nonlinear Studies, Los Alamos National Laboratory for their hospitality during the time when this work was performed.

References

[1] A. Einstein, in: Scientific papers presented to Max Born (Hafner, New York, 1953) p. 33.
[2] G.P. Berman and G.M. Zaslavsky, Physica A 91 (1978) 450.
[3] M. Toda and K. Ikeda, Phys. Lett. A 124 (1987) 165.
[4] G.M. Zaslavsky, Phys. Rep. 80 (1981) 157.
[5] M.V. Berry and N.L. Balazs, J. Phys. A 12 (1979) 625.
[6] H. Frahm and H.J. Mikeska, Z. Phys. B 60 (1985) 117.
[7] F. Haake, M. Kus and R. Scharf, Z. Phys. B 66 (1987) 381.
[8] K. Nakamura, A.R. Bishop and A. Shudo, Phys. Rev. B 39 (1989) 12422.
[9] B.V. Chirikov, F.M. Izrailev and D.L. Shepelyansky, Sov. Sci. Rev. C 2 (1981) 208.
[10] B.V. Chirikov, Chaos 1 (1991) 95.
[11] J.E. Bayfield and P.M. Koch, Phys. Rev. Lett. 33 (1974) 258.
[12] P.M. Koch, Rydberg states of atoms and molecules, eds. R.F. Stebling and F.B. Dunning (Cambridge Univ. Press, Cambridge, 1983).
[13] G. Casati, B.V. Chirikov, D.L. Shepelyansky and I. Guarnery, Phys. Rep. 154 (1987) 77.
[14] R.H. Dicke, Phys. Rev. 93 (1956) 99.

[15] R. Bonifacio and G. Preparata, Phys. Rev. A 2 (1970) 336.
[16] S. Stenholm, Phys. Rep. 6 (1973) 3.
[17] S. Haroche and J.M. Raimond, Adv. At. Mol. Phys. 20 (1985) 347.
[18] Yu.A. Sinitsin and V.M. Tsukernik, Phys. Lett. A 90 (1982) 339.
[19] O.B. Zaslavsky, Ukr. Fiz. Zh. 29 (1984) 419.
[20] G.P. Berman, E.N. Bulgakov and G.M. Zaslavsky, Chaos 2 (1992) 257.
[21] R.J. Glauber, Phys. Rev. 131 (1963) 2766.
[22] J.M. Radcliffe, J. Phys. A 4 (1971) 313.
[23] K.N. Alekseev and G.P. Berman, Sov. Phys. JETP 65 (1987) 1115.
[24] D.D. Holm, G. Kovačič and B. Sundaram, Phys. Lett. A 154 (1991) 346.
[25] D.D. Holm and G. Kovačič, Physica D 56 (1992) 270.
[26] L.G. Yaffe, Rev. Mod. Phys. 54 (1982) 407.
[27] A.N. Holden, C. Kittel and F.R. Yager, Phys. Rev. 77 (1950) 147.
[28] V.W. Cohen, C. Kikuchi and J. Turkevich, Phys. Rev. 85 (1952) 379.
[29] S.A. Altshuller and B.M. Kozirev, Electronic paramagnetic resonance (Fizmatgiz, Moscow, 1961).